ARTICLE OPEN

Check for updates

# Sex-specific GABAergic microcircuits that switch vulnerability into resilience to stress and reverse the effects of chronic stress exposure

Tong Jiang[1,2], Mengyang Feng[1,2,4], Alexander Hutsell[3] and Bernhard Lüscher[1,2,3]✉



Clinical and preclinical studies have identified somatostatin (SST)-positive interneurons as critical elements that regulate the vulnerability to stress-related psychiatric disorders. Conversely, disinhibition of SST neurons in mice results in resilience to the behavioral effects of chronic stress. Here, we established a low-dose chronic chemogenetic protocol to map these changes in positively and negatively motivated behaviors to specific brain regions. AAV-hM3Dq-mediated chronic activation of SST neurons in the prelimbic cortex (PLC) had antidepressant drug-like effects on anxiety- and anhedonia-like motivated behaviors in male but not female mice. Analogous manipulation of the ventral hippocampus (vHPC) had such effects in female but not male mice. Moreover, the activation of SST neurons in the PLC of male mice and the vHPC of female mice resulted in stress resilience. Activation of SST neurons in the PLC reversed prior chronic stress-induced defects in motivated behavior in males but was ineffective in females. Conversely, activation of SST neurons in the vHPC reversed chronic stress-induced behavioral alterations in females but not males. Quantitation of c-Fos$^+$ and FosB$^+$ neurons in chronic stress-exposed mice revealed that chronic activation of SST neurons leads to a paradoxical increase in pyramidal cell activity. Collectively, these data demonstrate that GABAergic microcircuits driven by dendrite targeting interneurons enable sex- and brain-region-specific neural plasticity that promotes stress resilience and reverses stress-induced anxiety- and anhedonia-like motivated behavior. The data provide a rationale for the lack of antidepressant efficacy of benzodiazepines and superior efficacy of dendrite-targeting, low-potency $GABA_A$ receptor agonists, independent of sex and despite striking sex differences in the relevant brain substrates.

*Molecular Psychiatry* (2025) 30:2297–2308; https://doi.org/10.1038/s41380-024-02835-8

## INTRODUCTION

Chronic and excessive amounts of stress are important vulnerability factors for virtually all psychiatric disorders, including especially major depressive disorder (MDD) and post-traumatic stress disorder (PTSD). These disorders are characterized by changes in negatively and positively regulated motivated behavior that manifest as heightened anxiety and anhedonia, respectively. Comparable changes in motivated behavior are observed in mice exposed to chronic stress. Brain volume loss and imaging studies of MDD patients point to the frontal cortex and hippocampus as primary sites of pathology [1]. At the molecular level, MDD and chronic stress are associated with diverse deficits in GABAergic inhibition that are reversed by multiple classes of antidepressants [2–4]. Molecular genetic studies in mice indicate that modestly reduced GABAergic inhibitory function, mainly in the hippocampus and cortex, results in HPA axis activation and anxiety- and anhedonia-like changes in motivated behavior [3, 5, 6]. Conversely, successful antidepressant drug treatments of patients and mice result in normalization of HPA axis function and GABA concentrations, along with restoration of impaired synaptic transmission [6–11], including reversal of the detrimental behavioral effects of chronic stress exposure [1]. Collectively, these studies in patients and mice suggest that impaired GABAergic inhibition in the hippocampus and cortex contributes causally to stress-associated psychiatric disorders, while antidepressants serve to reverse such deficits. By extension, these studies suggest that GABA itself has antidepressant drug-like properties that promote stress resilience [4, 12].

A separate body of work indicates that chronic stress and MDD are associated with reduced activity of frontal cortical output neurons [13] and diminished functional connectivity [14–16], while selective stimulation of pyramidal neurons (PNs) in the medial prefrontal cortex (mPFC) of mice mimics antidepressant drug treatment in that it reverses stress-induced defects in motivated behavior [17–20]. An essential question arising from these observations is whether GABAergic inhibition increases or reduces the activity of cortical output cells. Lastly, stress-sensitive psychiatric conditions in general and depressive disorders, in particular, show prominent sex differences in prevalence and disease-associated transcriptomes, which suggests that sex differences are involved in the mechanisms underlying successful antidepressant drug treatments [21, 22].

[1]Department of Biology, Pennsylvania State University, University Park, PA, USA. [2]Center for Molecular Investigation of Neurological Disorders (CMIND), The Huck Institutes of the Life Sciences, Pennsylvania State University, University Park, PA, USA. [3]Department of Biochemistry & Molecular Biology, Pennsylvania State University, University Park, PA, USA. [4]Present address: Picower Institute of Learning and Memory, Massachusetts Institute of Technology, Cambridge, MA, USA. ✉email: BXL25@psu.edu

Received: 12 May 2024 Revised: 1 November 2024 Accepted: 6 November 2024
Published online: 16 November 2024

Loss of function of GABAergic interneurons (INs), notably in the neocortex and hippocampus, is broadly implicated in stress-associated psychiatric disorder as evidenced by downregulation of markers for INs in MDD, bipolar disorder, and schizophrenia and chronic stress-induced downregulation of the same markers in rodents [23, 24]. GABAergic INs of the neocortex can be subdivided into three largely non-overlapping and similarly abundant subclasses based on the expression of the neuropeptide somatostatin (SST), the calcium-binding protein parvalbumin (PV), and the 5-HT3a receptor, respectively [25]. SST-expressing INs of the neocortex consist mainly of Martinotti cells that innervate the distal apical dendrites of PNs and modulate the strength of adjacent glutamatergic inputs to these cells. By contrast, PV INs inhibit the soma, proximal dendrites, and axon initial segments (AIS) of PNs, thereby exerting robust control over action potential firing. The majority of 5-HT3a receptor-expressing INs also express the vasointestinal peptide (VIP) and act via SST INs to disinhibit PNs [26]. Homologous IN classes, including dendrite targeting SST INs, are also present in the hippocampus [27, 28].

Preclinical and clinical studies point to a loss of dendritic spine synapses of pyramidal neurons (PNs) as primary defects in stress-associated mental disorders [29, 30]. These phenotypes point to a loss of dendritic inhibition by SST INs as a possible source of vulnerability. Indeed, SST mRNA and protein are downregulated by stress exposure in rodents and in postmortem brains of subjects with MDD [31]. Loss of SST neurons is also increasingly implicated in aging and Alzheimer's dementia, which are comorbid with MDD [24, 32], while maintenance of SST INs appears to be neuroprotective as evidenced by subjects with Alzheimer's pathology that have maintained high cognitive function [33]. In mice, a one-hour immobility stressor leads to a lasting increase in SST IN activity in the mPFC and a corresponding potentiation of inhibitory synaptic inputs to pyramidal cell dendrites [34]. Similar activity-induced long-term potentiation has been described for SST INs in the hippocampus [35]. Therefore, SST INs seem suited to exert a neuroprotective role that scales with short-term stress but gets overwhelmed under extreme or chronic stress conditions and in certain neuropathological conditions.

In testing whether selective potentiation of GABAergic inhibition at dendrites of PNs promotes stress resilience, we recently showed that genetically-induced global disinhibition of SST INs in mice (through deletion of an essential subunit of $GABA_A$ receptors from SST cells, SSTCre:$\gamma2^{f/f}$ mice) results in behavioral changes that mimic those of antidepressant drug treatment, as well as resilience to chronic stress-induced anxiety [36, 37]. Ex vivo slice recordings from SST INs in the cortex and hippocampus revealed a drastic (~80%) loss of inhibitory synaptic inputs to SST neurons and a large (~60% to 95%) increase in input resistance. Current clamp recordings from SST INs showed a corresponding increase in action potential firing that was reflected in significantly increased inhibitory synaptic inputs to PNs in both brain regions. Collectively, the data indicated that chronically enhanced excitability of SST INs and correspondingly enhanced GABAergic inhibition at dendrites of PNs facilitates anxiolytic- and antidepressant-like behavioral responses [36]. However, SST neurons are present throughout the brain and in diverse peripheral tissues, and we could not exclude a contribution to altered behavior by altered circuit development.

Here we asked whether the anxiolytic- and antidepressant-like behavioral phenotypes of SSTCre:$\gamma2^{f/f}$ mice can be reproduced by tonically increasing the excitability of SST INs in specific brain regions in adulthood, whether chronic stress-induced alterations in motivated behavior can be reversed by chronic activation of SST INs in specific brain regions, whether any of the results differed by sex, and whether and how a chronic increase in excitability of SST INs associated with antidepressant-like behavioral consequences affects the activity of their putative pyramidal target cells in vivo. We focused on the prelimbic cortex (PLC) and ventral hippocampus (vHPC) as brain regions that are highly stress-sensitive [29] and known to regulate synaptic excitation/inhibition balance-dependent positively and negatively regulated motivated behaviors.

## MATERIALS AND METHODS

### Animals

SSTCre (also known as *Sst* $^{tm2.1(cre)Zjh}$/J, stock #013044), PVCre (B6.Cg-*Pvalb*$^{tm1.1(cre)Aibs}$/J, stock No: 012358) mice and C57BL/6 J mice (BL6, stock No. 000664) were obtained from Jackson Laboratory (Bar Harbor, MN). SSTCre and PVCre breeder mice were maintained as heterozygotes and routinely backcrossed with wildtype 129×1/SvJ mice (RCC Ltd. Biotechnology and Animal Breeding, Füllinsdorf, Switzerland) and BL6 mice, respectively. The breeding colony was kept under a 12:12 h light–dark cycle, on corn cob bedding and with food and water ad libitum. Offspring were genotyped by PCR of tail biopsies at the time of weaning and then sorted into gang cages of 5–6 mice per cage under an inverted 12:12 h light–dark cycle. All animal experiments were approved by the Institutional Animal Care and Use Committees (IACUC) of the Pennsylvania State University and conducted per the guidelines of the National Institutes of Health (NIH).

### Chemogenetic manipulation

Stereotaxic surgeries were conducted on the mice at 8–10 weeks of age, with males and females staggered by approximately one week to allow for sequential behavioral testing. Cre transgenic mice were anesthetized with vaporized isoflurane/$O_2$ (5% initiation, 2% maintenance) and mounted on a stereotaxic frame (Stoelting, Wood Dale, IL). The surgical site was shaved and prepared with betadine, by scrubbing with ethanol, and with an injection of bupivacaine (4 mg/kg, s.c.). A scalp incision was made along the midline of the skull, the skin was pulled to the sides, and bilateral drill holes were made, targeting the prelimbic cortex (PLC, AP: 1.8 mm, ML: ± 0.4 mm, DV: 2.2–2.3 mm) or ventral hippocampus (vHPC, AP: −2.9 mm, ML: ± 2.9 mm, DV: 3.25 mm) [38]. Equal groups of Cre-transgenic mice balanced for weight and date of birth were injected bilaterally with Cre-dependent AAV vectors encoding a double-floxed Designer Receptor Exclusively Activated by Designer Drug (DREADD) construct fused to mCherry (pAAV-hSyn-DIO-hM3Dq(Gq)-mCherry, abbreviated here as hM3Dq, #0474-AAV5) or the double floxed control vector (Ctrl) carrying a cDNA for mCherry alone (pAAV5-hSyn-DIO-mCherry#50459-AAV5, Addgene, Watertown, MA), using 0.3 µL of virus per site at a titer of > 1–2 × $10^{13}$ vg/mL. The wound was closed with an absorbable polyglycolic acid suture (5/0, CP Medical 421A). The mice were allowed to recover for at least two weeks before the experiments were continued. The injection sites were examined at the end of experiments using immunofluorescence staining of floating sections for mCherry followed by confocal microscopy or scanning with an Odyssey® CLx imager (LI-COR, Lincoln, NE).

### Stress treatment

The mice were exposed to chronic variable stress (CVS) as described [39, 40], starting on day one with a tail suspension stressor, followed on day two with a restraint stressor, and on day three with exposure to foot shocks, which were then repeated for a total of 15 or 21 days. For tail suspension, the mice's tails were taped to a metal crossbar mounted 35 cm above the home cage for one hour. For the restraint stressor, the mice were placed into a perforated 50 ml Falcon® tube for one hour. Foot shock treatment involved exposure to 100 randomly distributed foot shocks (0.45 mA × 3 s) delivered within one hour, using a maximum of 10 mice per chamber of a two-compartment shuttle box (SanDiego Instruments, San Diego, CA) with the connecting gate closed. After each stressor, the mice were returned to their home cages.

### Treatment with clozapine-N-oxide (CNO)

CNO (NIMH Chemical Synthesis and Drug Supply Program) was dissolved at 100 mg/ml in dimethyl sulfoxide, diluted 1:1 with 0.9% saline and loaded into Alzet® mini pumps (Model 1004, DURECT Corp., Cupertino, CA) designed to release drug at a rate of 0.11 µl/h for up to 4 weeks. For a 25 g mouse, the resulting dose of CNO was calculated as 0.22 mg/kg/h. Minipumps were implanted on the animal's upper back between 14 and 28 days after virus injection and within a 7-day window for each

experiment. The area below the animal's neck was shaved, followed by anesthesia via isoflurane inhalation and a dose of bupivacaine (4 mg/kg, s.c.) at the surgical site. A skin incision was made, and the minipump was inserted into the surgical opening with the cap facing inward. Wound clips (SAI Infusion Technologies) used to close the wound were removed seven days post-surgery. For experiments that involved the removal of minipumps before behavioral testing, the mice were anesthetized as described, and an incision was made close to but not overlapping with the initial incision. The minipumps were then removed using sterile forceps, and the wounds were closed with wound clips.

### Behavioral testing

The mice were singly housed under an inverted 12:12 h light–dark cycle, starting one day before the start of behavioral testing, with the two sexes kept in separate rooms. Behavioral testing followed the time course indicated in the Figures, using one test per day and with the experimenter blinded to the type of virus injected. Testing was initiated ~3 h after the lights were turned off and was conducted under red light, except for the open field test (OFT). The elevated plus maze (EPM) apparatus [36] consisted of an elevated (40 cm) crossbar with two open and two closed arms (30 × 5 cm). The closed arms were surrounded by 20 cm walls of clear Plexiglas, and the edges of the open arms were raised by 2 mm to reduce accidental falling. At the start of the test, the mouse was placed into the center square of the maze, facing a closed arm. The behavior was video recorded for 5 min, and the numbers of open and closed arm entries and the open arm duration were automatically recorded using EthoVision XT13 (Noldus Information Technologies, Leesburg, VA). The OFT [36] was used to assess locomotion and behavioral inhibition in a novel arena exposed to bright light (75 lux). The OFT arena was divided evenly into a 5 × 5 grid, with the central 3 × 3 grid designated as the center of the arena. The mice were allowed to freely explore an opaque Plexiglas arena (50 × 50 × 20 cm) for 10 min. The behavior was video recorded, and the duration and frequency of entering the center were captured by EthoVision. For the forced swim test (FST) [36], the mice were placed into the 4 L beaker containing 3 L of 25 ± 1 °C water, and their activity was video recorded for 6 min. The frequency of inactivity, total duration spent inactive, and latency to the first inactivity during the last 5 min of the test were automatically recorded using EthoVision. Bouts of inactivity were set as an activity level ≤1.15% of the maximum and lasting ≥2 s. A z-scored mobility index that combined the three measures was computed as described [41]. For the novelty-suppressed feeding test (NSFT) [36], the mice were acclimated to an empty Petri dish in their home cage while being food-deprived on wood chip bedding for 18 h before testing. On test day, they were transferred to a corner of a novel test arena (50 × 40 × 12 cm) containing wood chip bedding. The latency to start feeding on a food pellet placed on a piece of cotton nesting square (6 × 6 × 0.5 cm) in the center of the arena was hand-scored for a maximum of 6 min even if no feeding had occurred. The mice were immediately returned to their home cages, which were supplemented with a dry food pellet placed on a Petri dish. The amount of food consumed during 30 min was recorded. The female urine sniffing test (FUST) [42] was used to assess changes in positively motivated, rewarding behavior in male mice. The mice were accustomed to a dry sterile cotton-tip applicator (Patterson Veterinary Supply, Saint Paul, MN) in their home cages (with lids removed) for 30 min and then exposed to a new water-soaked cotton tip for 3 min. After 45 min, they were exposed to a fresh female-urine-soaked cotton tip. The behavior was video-recorded, and the duration spent sniffing the urine-soaked cotton tip during the first 3 min was scored offline. The sucrose splash test (SSPT) was used to assess positively motivated, rewarding behavior in female mice [43, 44]. The mice were transferred briefly to an empty cage, and the fur coat on their back was sprayed with 1 mL of 20% sucrose solution using a spray bottle to stimulate grooming behavior. They were immediately returned to their home cage, and the grooming duration was recorded during the first 5 min using a stopwatch.

### Immunohistochemistry

To standardize the arousal state of the animals at the time of perfusion, each mouse was transferred to a novel gang cage for 10 min, followed exactly 80 min later by deep anesthesia with avertin (250 mg/kg) and transcardial perfusion with 4% paraformaldehyde in phosphate-buffered saline (PBS). The brains were postfixed overnight, and coronal sections (40 µm) were stored in PBS containing 0.02% $NaN_3$ at 4 °C until analysis. Immunostaining was performed in PBS supplemented with normal goat serum (2.5%), normal donkey serum (2.5%), 0.3% Triton X-100, and primary antibodies (1 h), followed by washing and incubation with appropriate secondary antibodies overnight. To monitor viral expression, sections were stained with rat anti-red fluorescent protein (RFP) (1:800, mAB 5F8, Chromotek) and then with IRDye® 800CW goat anti-rat secondary antibody (1:500, LI-COR). Sections mounted onto glass slides were imaged using an Odyssey® CLx scanner (LI-COR). For analyses of the density of c-Fos and FosB expressing neurons, the sections were immunostained with rat anti-RFP (1:800, Chromotek, recognizing mCherry) together with guinea pig anti-c-Fos (AB_2619946, 1:3000, SySy), monoclonal rabbit anti-FosB (1:2000, AB_184938, ABCAM) and rabbit anti-PV (AB_298032, 1:500, SySy) or chicken anti-PV (PA5-143579, 1:500, Invitrogen), followed by appropriate mixtures of secondary antibodies. The injection sites were imaged with a ZEISS® LSM 800 (20×/0.8 N.A objective). Z-stack images were captured from regions of interest (ROIs) of 300 × 300 pixels size and 10 µm depth; 6–14 ROIs were collected from 3–7 coronal sections per animal. The densities of c-Fos$^+$ and FosB$^+$ cells in collapsed z-stack images of each ROI were automatically quantified using the "analyze particle" function of ImageJ, with an intensity threshold of >60 and a particle size threshold of >30 pixels. The z-stacks were manually inspected to correct for overlapping undercounted cell counts. The densities of mCherry$^+$, PV$^+$, and double positive cells were quantified manually and examined visually in all three axes of Z-stack images to score for colocalization. The densities of c-Fos$^+$ and FosB$^+$ mCherry$^+$ cells in each image were normalized to the density of mCherry$^+$ cells in the same images to adjust for variability in the infection density.

### Statistics

Statistical testing was performed using Prism 10 software (GraphPad, La Jolla, CA). Simple two-sample comparisons were done by two-sided t-test or, if the data failed the normality test (Anderson–Darling), by Mann–Whitney test. Multiple comparisons were made by 2-way ANOVA followed by Sidak's post hoc test. Data from mistargeted mice and from mice that escaped the maze during behavioral testing, and statistical outliers (ROUT method, Q = 1%) were removed from analyses. Removal of outliers didn't affect the significance of any of the results.

## RESULTS

### Chronic activation of SST neurons in the prelimbic cortex has anxiolytic- and antidepressant-like effects on motivated behavior in male but not female mice

We previously showed that global disinhibition of SST INs in SSTCre:γ2$^{f/f}$ mice results in behaviors that mimic the effects of antidepressant drug treatment in both male and female mice [36]. SST neurons in SSTCre:γ2$^{f/f}$ mice are hyperexcitable due to the loss of GABAergic inhibitory synaptic input and a significant increase in input resistance [36]. Moreover, SST neurons are present throughout the brain as well as in diverse peripheral tissues, and this mutation is induced during embryonic development. To address this question, we injected the prelimbic cortex (PLC) of male SSTCre mice (8–10 weeks of age) with a Cre-dependent AAV-hM3Dq-mCherry vector (hM3Dq) or a Cre-dependent AAV-mCherry control vector (Ctrl) and, after allowing two to three weeks for virus expression, implanted all animals with clozapine-N-oxide (CNO)-releasing osmotic minipumps, regardless of virus injected. We aimed to mimic the hyperexcitability of SST neurons observed in SSTCre:γ2$^{f/f}$ mice in AAV-hM3Dq-manipulated SSTCre mice with a low but constant dose of CNO (~0.22 mg/kg/h). Behavioral testing of male mice was initiated 12 days after minipump insertion and continuous CNO exposure using the test sequence depicted in Fig. 1A and sFig. 1A. We used the EPM, OFT, and NSFT to assess changes in locomotion and negatively regulated anxiety-related behavior under low and comparatively high acute stress conditions, respectively. In addition, we used the FUST to evaluate changes in positively regulated motivated behavior and hedonic drive in male mice. The sniffing of urine in this test is associated with dopamine release in the nucleus accumbens, indicating that it is rewarding [45]. Finally, these initial experiments included the FST as a test traditionally used to assess antidepressant drug activity in rodents. The behavior of PLC-injected male mice in the EPM (Fig. 1B) and OFT (sFig. 1B) was unaffected by hM3Dq/CNO-mediated chronic activation of SST cells, indicating unaltered locomotion and anxiety-related behavior under the low acute stress conditions of the EPM and

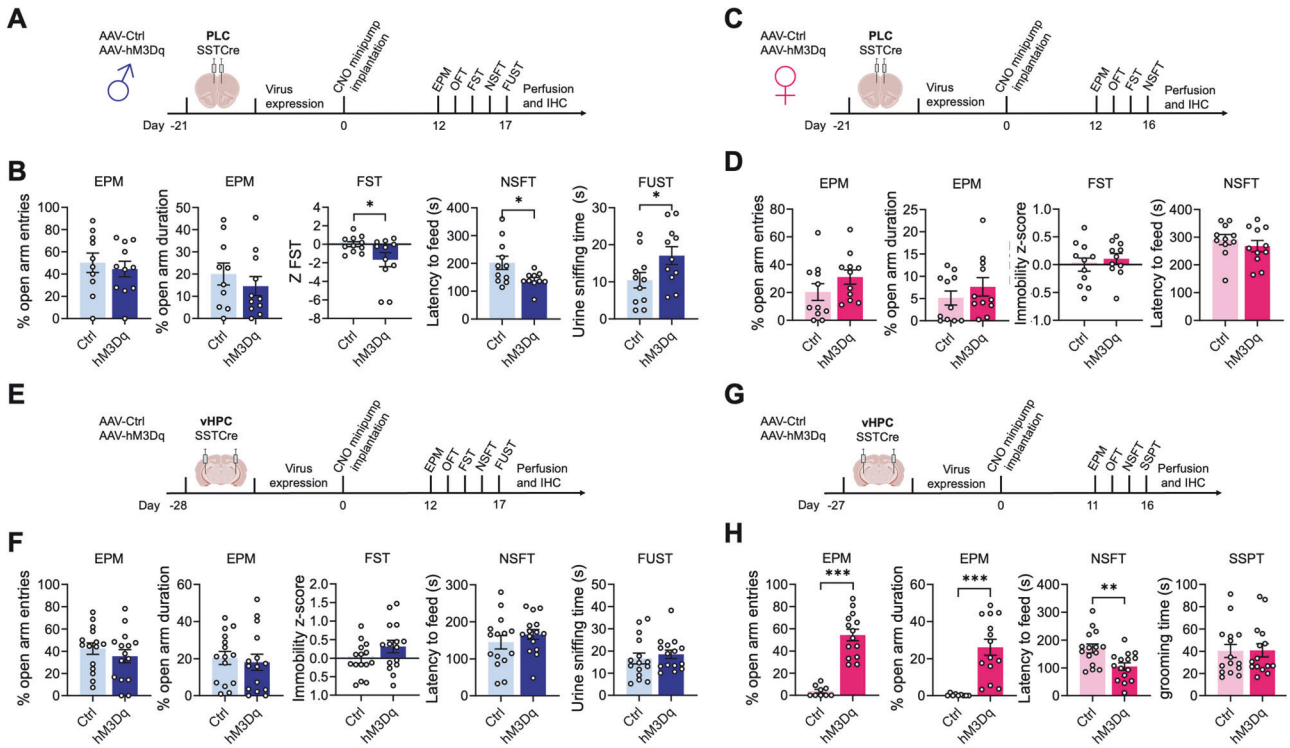


**Fig. 1 Chronic activation of SST neurons induces antidepressant-like changes in motivated behavior via sex-specific brain substrates.** Chemogenetic manipulation of PLC-injected male (**A**, **B**) and female (**C**, **D**) SSTCre mice, including experimental designs (**A**, **C**) and results from the EPM, FST, and NSFT (both sexes) and FUST for males (**B**, **D**). hM3Dq-mediated chronic activation of SST INs reduced the immobility z-score in the FST (n = 11, 11, $p < 0.05$, t = 2.09) and the latency to feed in the NSFT (n = 11, 10, $p < 0.05$, t = 2.34), and increased the urine sniffing time in the FUST of male mice (n = 11, 11, $p < 0.05$, t = 2.12) (**B**) but had no effect in the NSFT and FST of females (n = 11, 11) (**D**). The two measures in the EPM were unaffected independent of sex (male, n = 10, 11; female, n = 11, 11) (**B**, **D**). **E**–**H** Analogous manipulation of male (**E**, **F**) and female (**G**, **H**) mice in the vHPC. hM3Dq-mediated activation of SST INs in the vHPC had no effect in males in all five tests (**F**) (n = 15, 15, t-tests) but increased the percent open arm entries (n = 9, 14, $p < 0.001$, t = 7.52) and times on open arms (n = 9, 14, $p = 0.001$, t = 4.76) and reduced the latency to feed in the NSFT in female mice (n = 11, 11, $p < 0.01$, t = 3.11). The SSPT was unaffected by SST IN activation (n = 15, 15). Data represent means ± SEM. *$p < 0.05$, **$p < 0.01$, ***$p < 0.001$, t-test.

OFT. However, in the FST and NSFT, hM3Dq injected mice showed a reduced immobility score and a reduced latency to feed, while in the FUST, they spent more time sniffing urine than did the empty vector Ctrls. Thus, chronic activation of SST neurons in the PLC of male mice resulted in antidepressant drug-like changes in both positively and negatively regulated forms of motivated behavior. Anxiolytic-like effects in the NSFT but not the EPM and OFT indicate that in these unstressed mice, SST neuron-mediated inhibition leads to anxiolysis selectively under comparatively high-stress test conditions.

Next, we tested the effects of PLC SST neuron activation in female mice (Fig. 1C, D, sFig. 1C, D). Behavior in the EPM and OFT was unaffected, as was the case in males (Fig. 1D, sFig. 1D). However, female mice differed from males in that activation of SST cells in the PLC had no effects in the NSFT and FST. This finding was unexpected because SSTCre:$\gamma 2^{f/f}$ mice with disinhibited SST neurons exhibit anxiolytic and antidepressant-like changes in behavior independent of sex [46]. The data suggested that GABAergic control of motivated behavior in the PLC is male-specific and that GABAergic control of motivated behavior in female mice is controlled by a different brain substrate.

### Chronic activation of SST neurons in the ventral hippocampus has anxiolytic-like effects on motivated behavior in female but not male mice

In search of a substrate for SST neuron-mediated changes in motivated behavior in female mice, we next focused on the ventral hippocampus (vHPC), a second major brain region implicated in the top-down control of motivated behavior [47, 48] (Fig. 1E–H, sFig. 1E–H). Interestingly, we found that the sex-specific effects of hM3Dq/CNO-mediated activation of SST neurons in the vHPC were opposite to those in the PLC, as indicated by the lack of an effect of SST neuron activation in the EPM, FST, NSFT, and FUST of male mice (Fig. 1E, F), and robust anxiolytic-like changes in the EPM and NSFT of female mice (Fig. 1G, H). As a substitute for the FUST and FST, we subjected vHPC-manipulated female mice to an SSPT. Grooming behavior in this test is accompanied by dopamine release in the nucleus accumbens [44], which indicates that the behavior is rewarding similar to sniffing female urine in male mice. However, the behavior of hM3Dq/CNO manipulated female mice in the SSPT was unaffected in this experiment (sFig. 1H). In retrospect, this finding is consistent with recent evidence that dopamine release and grooming behavior in this test are selectively stimulated after chronically stressful experiences [44], as we confirmed further below. Notably, the anxiolytic-like effect of SST neuron activation in the vHPC of females was seen both with tests involving low acute stress (EPM) and high acute stress conditions (NSFT), whereas in PLC-manipulated male mice, it was only seen under high acute stress conditions (NSFT), seemingly reflecting greater baseline behavioral inhibition in the EPM of females compared to males. The behavior in the OFT was unaffected, independent of sex and brain region manipulated (sFig. 1). Moreover, home cage feeding of food-deprived vHPC-manipulated animals was unaffected, indicating that the behavioral changes in the NSFT were not due to an altered feeding drive. Collectively, these experiments indicated a striking sex-specific dissociation in the top-

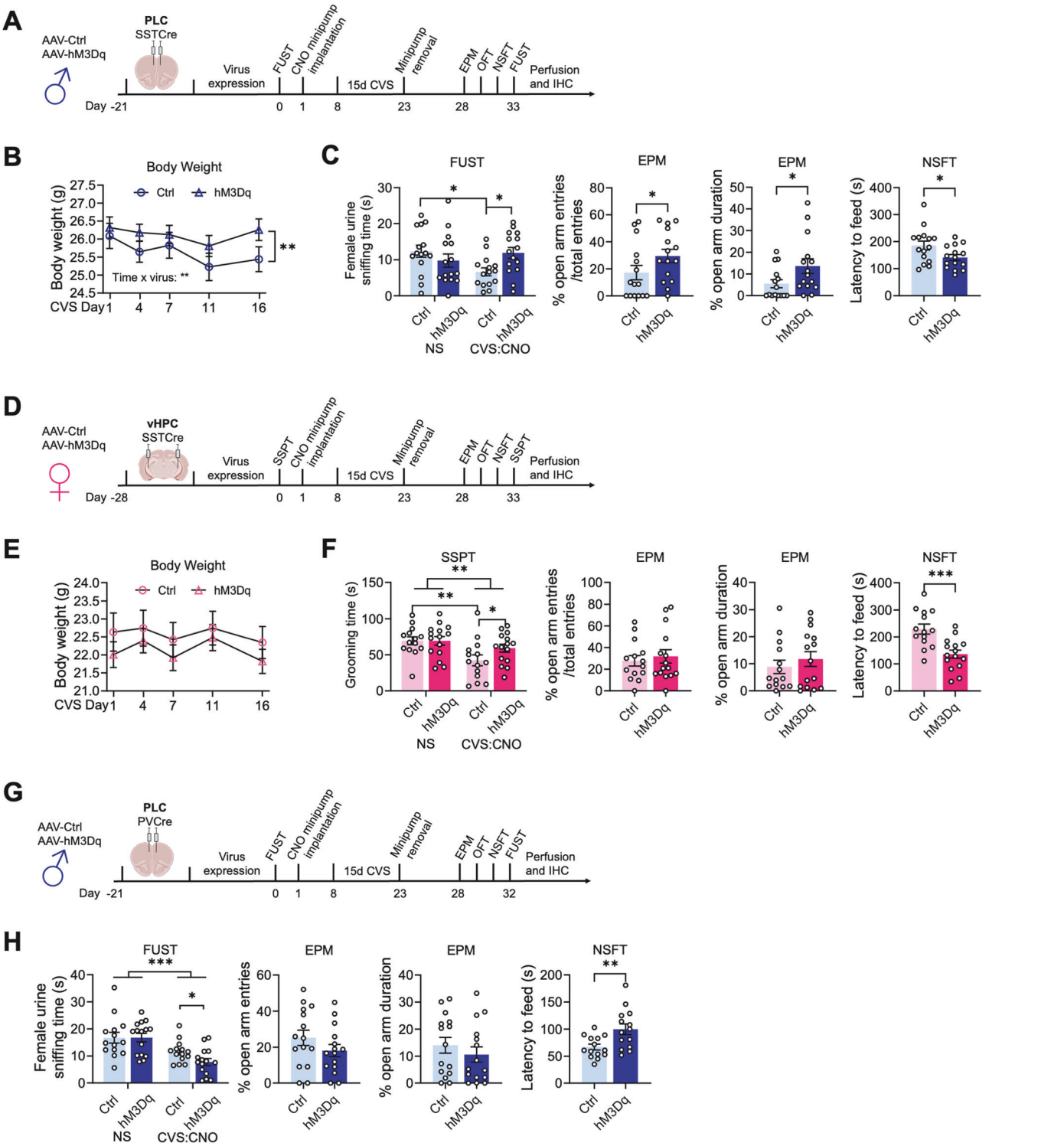


down control of antidepressant- and anxiolytic-like motivated behavior by prelimbic and hippocampal GABAergic microcircuits.

**SST neurons in the PLC and vHPC mediate resilience to chronic stress-induced defects in motivated behavior in male and female mice, respectively**

We next asked whether the activation of SST INs in the PLC of male mice is sufficient to confer resilience to chronic stress-induced defectsicits in motivated behavior. Virus-transduced mice were allowed to recover and subjected to an initial FUST to assess baseline behavior, followed by CNO minipump implantation, 15 days of CVS, minipump removal, and a battery of tests assessing negatively and positively motivated behavior, including a second FUST (Fig. 2A). The weights of the mice during the three weeks of CVS exposure were measured to assess the effects of chronic stress on whole-body physiology (Fig. 2B). Interestingly, CVS resulted in a time-dependent body weight reduction in Ctrl but not hMD3q-injected mice, suggesting

**Fig. 2 Activation of SST but not PV neurons induces resilience to chronic stress-induced changes in motivated behavior.** Time courses of manipulations of male (**A**) and female SSTCre mice (**D**) and male PVCre mice (**G**). The mice were injected with hM3Dq or Ctrl virus in the brain region indicated, followed by the analysis of baseline behavior in a FUST [males (**A**, **G**)] or a SSPT [females (**D**)], implantation of CNO minipumps, exposure to 15 days of CVS, removal of minipumps, and testing in the EPM, OFT, NSFT, and a second FUST or SSPT. **B** The weight of PLC-injected male mice showed a time× virus interaction ($F_{(4, 112)} = 3.7$, $p < 0.01$, RM ANOVA) with a time-dependent weight loss in Ctrl- but not hM3Dq-injected mice during CVS (n = 15, 15, $p < 0.01$). **C** A comparison of the female urine sniffing times between the first and second FUST revealed a stress x vector interaction ($F_{(1,28)} = 7.4$, $p < 0.05$, RM ANOVA) that was significant for Ctrl- (n = 15, 15, $p < 0.05$,) but not hM3Dq-injected mice (n = 15, 15, $p = 0.52$). The hM3Dq- vs. Ctrl-injected, CVS-exposed and CNO-treated mice showed a greater urine sniffing time (n = 15, 15, $p < 0.05$). In the EPM and NSFT, hM3Dq- vs. Ctrl-injected CNO- and CVS-exposed mice showed anxiolytic-like changes in motivated behavior with respect to percent open arm entries (n = 15, 15, $p < 0.05$, U = 63.5) and percent open arm duration (n = 15, 15, $p < 0.05$, U = 65)] and latency to feed (n = 15, 15, $p < 0.05$, t = 2.22). **E** vHPC-injected female mice exposed to CVS showed no measurable change in body weight independent of the vector injected. **F** The time spent grooming in the SSPT showed an overall stress effect ($F_{(1, 27)} = 9.799$, $p < 0.01$, RM ANOVA) with a reduction in Ctrl- (n = 14, 14, $p < 0.01$) but not hM3Dq-injected mice (n = 15, 15, $p = 0.41$). A planned comparison of grooming times after CVS showed increased grooming duration in hM3Dq- vs. Ctrl-injected mice (n = 14, 15, $p < 0.05$, t = 1.83). In the NSFT, hM3Dq-injected mice showed a shorter latency to feed than Ctrl-injected mice (n = 14, 15, $p < 0.001$, t = 3.96). The percent open arm entries and open arm times in the EPM of CVS-exposed mice were unaffected by virus treatment (n = 14–15). **G** Analyses of PVCre male mice injected in the PLC analogous to SSTCre males in (**B**) and (**C**). **H** In the FUST, a comparison of the urine sniffing times before and after CVS showed a stress effect independent of the vector injected ($F_{(1, 27)} = 33.96$, $p < 0.001$, RM ANOVA). A planned comparison of Ctrl- and hM3Dq-virus-injected mice after CVS exposure revealed a reduction in the urine sniffing time in hM3Dq- vs. Ctrl-injected mice (n = 14, 15, $p < 0.05$, t = 2.43). The percent open arm entries and open arm times in the EPM of CVS-exposed mice remained unaffected by virus treatment (n = 15, 15). However, in the NSFT, hM3Dq- vs. Ctrl-injected mice showed an anxiogenic-like increase in the latency to feed (n = 14, 14, $p < 0.01$, t = 2.94). Data represent means ± SEM, *$p < 0.05$, **$p < 0.01$, ***$p < 0.001$, 2-way ANOVA plus Sidak test, Mann Whitney, or t-test.

whole-body physiological stress protection. Repeated testing in the FUST before and after CVS revealed an overall stress effect independent of the virus injected, as well as an interaction between CVS and the type of virus injected. CNO reversed the CVS effect in hM3Dq but not Ctrl virus-manipulated mice (Fig. 2C). Analyses after CVS exposure further showed that hM3Dq-mediated activation of SST neurons had anxiolytic-like effects on open arm entries and open arm duration in the EPM, and latency to feed in the NSFT. Collectively, these data indicated that SST INs in the PLC were sufficient to mediate resilience to CVS-induced defects in both positively and negatively regulated behaviors in male mice.

Next, we similarly tested whether SST INs in the vHPC confer stress resilience in female mice (Fig. 2D). In contrast to males, CVS did not affect the weight of female mice, independent of DREADD manipulation (Fig. 2E). Despite this qualitative sex difference in the stress effect, comparing the behavior in the SSPT before and after CVS revealed a significant main effect of CVS (Fig. 2F, first panel). Post hoc analyses showed that this effect was significant in Ctrl- but not hM3Dq-injected mice. Similar to PLC-manipulated males, hM3Dq-injected female mice exhibited an anxiolytic effect in the NSFT (Fig. 2F, fourth panel). Therefore, SST neurons in the vHPC mediate resilience to CVS-induced defects in positively and negatively regulated behavior in female mice. Notably, SST neuron activation in the vHPC of females did not affect the percentage of open arm times and open arm entries in the EPM (Fig. 2F, second and third panels), in contrast to SST neuron activation in the PLC of males (Fig. 2C), and behavior in the OFT and home cage feeding of food-deprived mice was unaffected, independent of sex, brain region, and IN type (sFig. 2A–F). These experiments suggest that the brain regions that mediate sex-specific antidepressant-like behavioral effects in the absence of stress also confer resilience to the detrimental behavioral consequences of chronic stress exposure. In male mice, GABAergic PLC-mediated stress resilience extends to stress-induced weight loss, whereas in female mice, this parameter could not be addressed due to the absence of a significant stress effect.

### Chronic activation of parvalbumin-positive INs in the PLC has detrimental effects in male mice

Unlike the pro-resilience function of SST neurons in the PLC of male mice, increased activity of parvalbumin (PV)-positive INs may have detrimental effects, as shown by others for the mPFC of female mice and hippocampus of males [49, 50]. To assess the function of PV neurons in the PLC of male mice, we evaluated the behavioral consequences of chemogenetic PV IN activation in CVS-exposed mice. As expected, a comparison of the female urine sniffing times before and after CVS revealed a significant stress effect independent of the virus injected. However, in contrast to the pro-resilience effect of PLC SST neuron activation (Fig. 2C), activation of PLC PV neurons exacerbated the CVS effect and led to a reduction in the sniffing time in hM3Dq vs. Ctrl vector-injected, CVS-exposed mice (Fig. 2H). Moreover, in contrast to the anxiolytic-like effect of PLC SST neuron activation in the NSFT (Fig. 2C), activation of PLC PV neurons during CVS exposure had anxiogenic-like effects, as evidenced by the additional increase in the latency to feed in hM3Dq vs. Ctrl virus-injected mice (Fig. 2H). Thus, the pro-resilience effect of GABAergic inhibition is specific to dendrite targeting GABAergic inhibition and is not observed with PV IN-mediated inhibition, which targets the somatodendritic compartment and AIS of PNs. Notably, the behaviors of hM3Dq-transduced PVCre mice in the EPM (Fig. 2H) and OFT (sFig. 2F) were unaltered, suggesting that the anxiogenic-like effects of PV neuron activation are manifested selectively under acutely stressful conditions.

### SST neurons in the PLC and vHPC act sex-specifically to reverse chronic stress-induced defects in motivated behavior in male and female mice, respectively

We next asked whether activation of SST neurons in the PLC would reverse prior CVS-induced defects in motivated behavior. Male mice transduced with hM3Dq or Ctrl virus were subjected to an initial FUST to assess baseline behavior, followed by three weeks of CVS and a second FUST to verify the stress effects (Fig. 3A). We then implanted CNO minipumps, followed 12 days later with a final behavioral test battery, including a third FUST. To prevent the possible fading of stress effects during the extended time course of experimentation, we preceded the final behavioral assessment with three days of CVS exposure, which by itself does not affect motivated behavior [40]. Comparison of PLC Ctrl and hM3Dq vector-injected mice in the FUST before CNO treatment revealed an overall effect of stress independent of the vector injected (Fig. 3B, 1st panel). Comparison of CVS-exposed mice before and after CNO treatment in the second and third FUST revealed an overall effect of CNO with a significantly greater female urine sniffing time in hM3Dq- vs. Ctrl-injected mice (Fig. 3B, 2nd panel). Thus, chronic activation of PLC SST neurons effectively reversed the anhedonia-like consequences of CVS exposure. The behavior in the EPM and OFT remained unaffected, indicating unaltered locomotion and anxiety-related behavior under low-

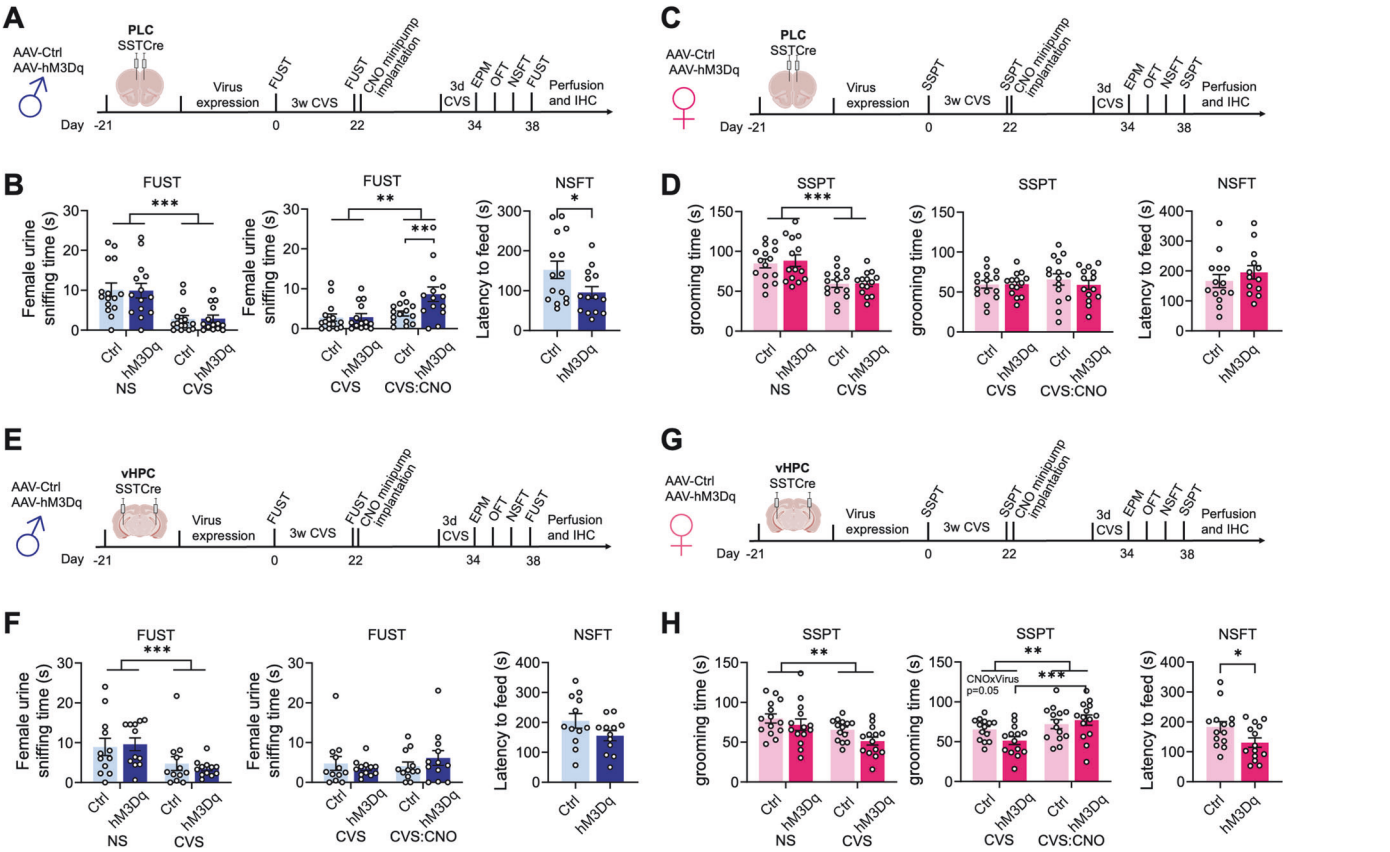


**Fig. 3 Activation of SST neurons reverses the behavioral effects of chronic stress exposure through sex-specific brain substrates.** Time courses of manipulations of male (**A**, **E**) and female SSTCre mice (**C**, **G**). The mice were injected with hM3Dq or Ctrl virus in the brains region indicated, followed by analysis of baseline behavior in a FUST [males (**A**, **E**) or SSPT (females (**C**, **G**)], exposure to 21 days of CVS, a second FUST or SSPT, respectively, implantation of CNO minipumps, three days of CVS, and testing in the EPM, OFT, NSFT, and a third FUST or SSPT, respectively. **B** A comparison of female urine sniffing times of PLC-injected male mice in sequential FUSTs before and after CVS revealed an overall stress effect ($F_{(1,27)} = 35.96$, $p < 0.001$, RM ANOVA) independent of vector injected. A comparison of the female urine sniffing times of CVS-exposed mice before and after CNO revealed an overall CNO effect ($F_{(1,27)} = 9.399$, $p < 0.01$) and a vector x CNO interaction ($F_{(1,27)} = 4.640$, $p < 0.05$, RM ANOVA). CNO increased the urine sniffing time in hM3Dq- vs. Ctrl-injected mice (n = 15, 14, $p < 0.01$). The latency to feed of hM3Dq- vs. Ctrl-injected was reduced (n = 15, 14, $p < 0.05$, t = 2.13). **D** Comparing the grooming times of PLC-injected female mice in sequential SSPTs before and after CVS revealed an overall stress effect ($F_{(1,27)} = 25.07$, $p < 0.001$, RM ANOVA). CNO did not affect the grooming time independent of the vector (n = 15, 14). The latency to feed in the NSFT after CVS and CNO was unaffected (n = 15, 14). **F** Comparing the female urine sniffing times of vHPC-injected male mice before and after CVS revealed an overall stress effect ($F_{(1,22)} = 19.55$, $p < 0.001$, RM ANOVA) independent of the vector injected. CNO did not affect the grooming time independent of the vector (n = 12, 12). The latency to feed was unaffected by the vector injected (n = 12, 12). **H** Comparing the grooming times of vHPC-injected female mice in sequential SSPTs before and after CVS revealed an overall stress effect ($F_{(1,26)} = 11.74$, $p < 0.01$, RM ANOVA). Comparing the grooming times of the CVS-exposed mice before and after CNO revealed an overall CNO effect and a CNO x vector interaction ($F_{(1,26)} = 4.064$, $p = 0.05$, RM ANOVA). CNO increased the grooming time of CVS-exposed hM3Dq- (n = 14, 14, $p < 0.001$) but not Ctrl-injected mice (n = 14, 14, $p = 0.34$). The latency to feed after CVS and CNO exposure of hM3Dq- vs. Ctrl-injected was reduced (n = 14, 14, $p < 0.05$, t = 2.17). Data represent means ± SEM, $^*p < 0.05$, $^{**}p < 0.01$, $^{***}p < 0.001$, 2-way ANOVA, Sidak, or t-test.

stress conditions (sFig. 3A, B). However, the latency to feed in the NSFT (a comparatively high-stress situation) was significantly reduced in hM3Dq vs. Ctrl vector-injected mice, indicating a reversal of stress-induced anxiety-like behavior. The home cage feeding of hM3Dq-injected mice was reduced, indicating that the change in the latency to feed was not explained by an altered feeding drive (sFig. 3B, last panel).

Analogous testing of female mice and substitution of the SSPT for the FUST and comparison of the grooming time before and after CVS exposure revealed a significant stress effect independent of the vector injected (Fig. 3C, D, first panel). However, CNO did not affect the grooming time, independent of the vector injected (Fig. 3D, 2nd panel). Similarly, a pairwise comparison of Ctrl- and hM3Dq-injected mice after CVS and CNO exposure in the NSFT revealed no difference between Ctrl- and hM3Dq-injected mice. Therefore, in contrast to male mice, activation of SST neurons in the PLC of female mice failed to reverse CVS-induced anhedonia- and anxiety-like behavior. Notably, the OFT and EPM behavior was unaltered and consistent with unaltered locomotion (sFig. 3C, D).

The findings thus far suggested that similar to effects on motivated behavior in the absence of stress, the reversal of chronic stress effects by GABAergic inhibition is sex and brain region-specific. To further examine this, we tested the ability of GABAergic circuits in the vHPC to reverse the effects of prior stress exposure (Fig. 3E, F). We injected the vHPC of SSTCre mice with Ctrl or hM3Dq virus, exposed the mice to CVS, and then implanted CNO-releasing minipumps (Fig. 3E). A comparison of male mice in the FUST before and after CVS exposure revealed an overall stress effect, independent of the virus transduced, as expected (Fig. 3F, first panel). However, in contrast to manipulations of the PLC, CNO exposure of hM3Dq-injected animals failed to reverse the CVS effect (Fig. 3F, 2nd panel). Similarly, a comparison of Ctrl- and hM3Dq-injected mice after CVS and CNO exposure failed to show

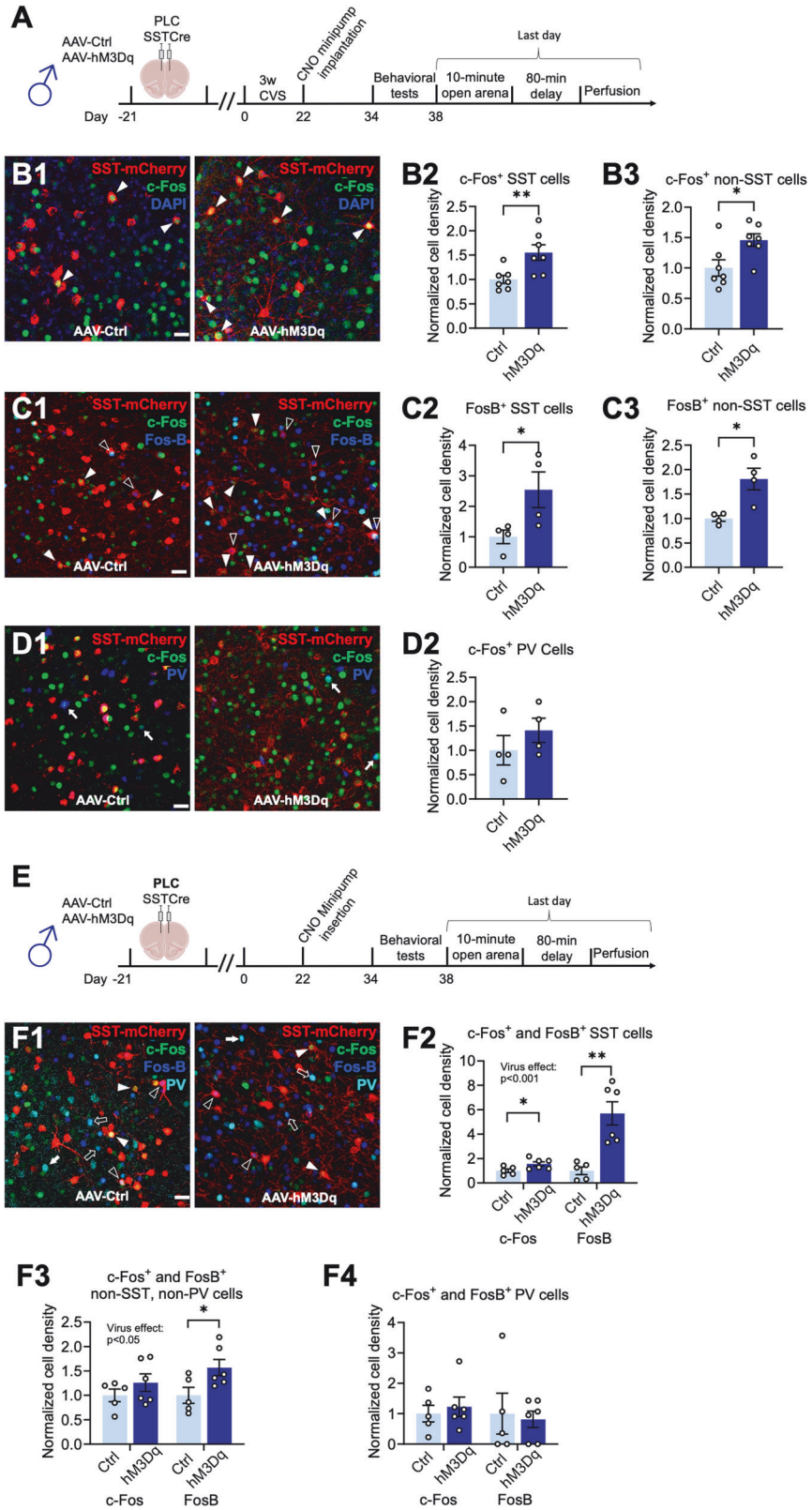


anxiolysis in the NSFT of hM3Dq-injected mice (Fig. 3F, 3rd panel). By contrast, analogous testing of female mice injected in the vHPC (Fig. 3G) and analyzed in the SSPT revealed a significant CVS effect that was reversed by CNO exposure selectively in hM3Dq- but not Ctrl-injected mice (Fig. 3H, 1st and 2nd panel). Moreover, testing in the NSFT revealed an anxiolytic-like effect of CNO in hM3Dq- vs. Ctrl-injected mice (Fig. 3H, 3rd panel). Thus, the reversal of chronic stress-induced anxiety and anhedonia-like behavior in male and female mice mediated by GABAergic microcircuits involves distinct cortical substrates.

**Fig. 4 hM3Dq-mediated activation of SST INs in the PLC increases the density of c-Fos and FosB immuno-positive PNs. A** Time course of manipulations. One day after the last day of behavioral testing, the mice were exposed to a novel open arena for minutes, and the brain perfused 80 min later. **B** Triple immuno-staining for virus-expressing SST INs (mCherry, red), c-Fos (green), and the nuclear stain, 4′,6-diamidino-2-phenylindole (DAPI, blue), with micrographs representative of Ctrl- (left) and hM3Dq- (right) injected animals (**B1**) and summary data showing increased densities of c-Fos$^+$ SST INs (B2, n = 7, 7, $p < 0.01$, t = 3.07) and c-Fos$^+$ non-SST neurons (n = 7, 7, $p < 0.01$, t = 2.69) in hM3Dq- vs. Ctrl-injected mice. **C** Triple staining for SST INs (mCherry$^+$, red), c-Fos (green), and FosB (blue) with representative micrographs of a Ctrl- (left) and hM3Dq-injected animals (right) (**C1**) and summary data showing increased densities of FosB$^+$ SST INs (n = 4, 4, $p < 0.05$, t = 2.48) (**C2**) and FosB$^+$ non-SST neurons (n = 4, 4, $p < 0.05$, t = 3.57) (**C3**) in hM3Dq- vs. Ctrl-injected mice. **D** Triple staining for SST INs (mCherry, red), c-Fos (green), and PV-INs (blue) with representative micrographs of Ctrl- (left) and hM3Dq-infected animals (right) (**D1**) and summary data showing unaltered densities of c-Fos$^+$ PV cells (n = 4, 4) (**D2**). The densities of c-Fos$^+$ and FosB$^+$ SST INs were normalized to the total densities of virally transduced mCherry$^+$ SST cells. **E** Experimental design as in (**A**) but without CVS exposure. **F** Quadruple immuno-staining for virus-expressing SST INs (mCherry, red), c-Fos (green), FosB (blue), and PV INs (teal), with micrographs representative of Ctrl (left) and hM3Dq (right) PLC-injected animals (**F1**) and summary statistics for c-Fos$^+$ and FosB$^+$ mCherry-labeled SST INs and putative PNs lacking SST and PV expression (**F2**). The hM3Dq-injected animals showed a significant increase in the density of c-Fos$^+$ and FosB$^+$ mCherry-positive SST cells ($F_{(1,18)} = 22.06$, $p < 0.001$). Post hoc tests showed significant virus effects for both c-Fos- (n = 5, 6, $p < 0.05$) and FosB-labeled cells (n = 5, 6, $p < 0.01$) (**F2**). The densities of mCherry and PV double-negative putative PNs that colocalized with c-Fos and FosB were increased in hM3Dq- vs Ctrl-injected animals ($F_{(1,18)} = 6.28$, $p < 0.05$) with a significant effect for FosB- (n = 5, 6, $p = 0.05$) but not c-Fos-colocalized cells (n = 5, 6, $p = 0.49$) (**F3**). The densities of c-Fos$^+$ PV INs and of FosB$^+$ PV INs were unaltered) ($F_{(1,18)} = 0.0023$, $p = 0.96$) (F4). Solid white arrowheads (**B1**, **C1**, **D1**, **F1**) point to c-Fos$^+$, mCherry$^+$ doubly positive cells; empty arrowheads (**C1**, **F1**) point to FosB$^+$ mCherry$^+$ doubly positive cells. Solid white arrows (**D1**) point to c-Fos-positive PV INs, and empty arrows point to c-Fos FosB doubly positive putative PNs. Scale bars, 30 μm. Data represent means ± SEM, *$p < 0.05$, **$p < 0.01$, ***$p < 0.001$, 2-way ANOVA, Sidak, or t-test.

### SST neuron-mediated reversal of CVS effects on motivated behavior involves increased activity of pyramidal cells

GABAergic synaptic transmission is widely known to inhibit glutamatergic depolarizing inputs and, hence, to reduce dendritic spiking and output of glutamatergic target neurons [51]. By contrast, all evidence suggests that antidepressant drug-like changes in motivated behavior involve increased rather than reduced activity of cortical output neurons [17, 19, 20]. We hypothesized, therefore, that chronically and modestly elevated GABAergic transmission at dendrites may lead to increased rather than reduced activity of pyramidal target cells. To test this prediction, we quantitated the densities of c-Fos- and FosB-expressing neurons as proxies for cell-specific neural activity in vivo. Male mice that had been transduced with AAV-hM3Dq or Ctrl virus in the PLC, followed by CVS exposure and CNO-induced reversal of behavioral stress effects (Figs. 3A and 4A), were subjected to immunostaining for c-Fos and virus-encoded, Cre-dependent mCherry to assess the density of c-Fos$^+$ and mCherry$^+$ doubly positive cells representing SST INs, as well c-Fos$^+$ non-SST (mCherry-negative) cells representative of PNs in areas exhibiting virally transduced SST cells. Precisely 90 min before euthanasia, the mice were exposed to a novel arena for 10 min to induce a mild but behaviorally relevant arousal state (Fig. 4A). The density of c-Fos$^+$ SST neurons was increased in hM3Dq- compared to Ctrl virus-transduced mice, which confirms that chronic low-level CNO-delivery increased the activity of hM3Dq expressing SST neurons (Fig. 4B1, B2) with 18.7% and 29.0% of mCherry-positive SST neurons showing c-Fos expression in Ctrl and hM3Dq injected mice, respectively. Significantly, the density of c-Fos$^+$ non-SST (mCherry-negative) cells was increased in parallel (Fig. 4B3), indicating that chronically increased inhibition by SST cells leads to paradoxically increased activation of non-SST cells. The density of c-Fos$^+$ PV$^+$ cells was less than 5% of the density of c-Fos$^+$ non-SST cells, indicating that c-Fos$^+$ non-SST cells consist predominantly of pyramidal cells. To corroborate these findings, we quantitated the density of mCherry$^+$ SST IN expressing FosB, a marker that is induced by neuronal depolarization and $Ca^{2+}$ entry similar to c-Fos but with a slower and longer-lasting time course [52]. The density of FosB$^+$ SST cells was greater in hM3Dq-injected mice than in. Ctrl-injected mice, with 7.9% and 20.2% of SST neurons showing expression of FosB in Ctrl- and hM3Dq virus-injected mice, respectively (Fig. 4C). These data confirmed that our chemogenetic strategy to modestly increase the activity of SST neurons was working as intended. Moreover, the density of FosB$^+$ non-SST cells was increased in hM3Dq vs. Ctrl-injected mice (Fig. 4C), confirming that SST IN activity increased the activity of their putative pyramidal target cells.

Optogenetic stimulation of the large majority of cortical SST neurons results in inhibition of pyramidal cells [53]. However, a small subset of SST$^+$ neurons in cortical layer IV has been shown to predominantly inhibit PV$^+$ cells [53], which raised the question of whether the SST IN-mediated activation of PNs reported here involved disinhibition via PV cells. We found that the density of c-Fos and PV double-positive neurons was unaltered (Fig. 4D), indicating that SST IN-mediated activation of PNs cannot be explained by PV IN-mediated disinhibition. It follows that the antidepressant-like, SST IN-mediated reversal of chronic stress-induced changes in motivated behavior can only be explained by direct SST IN-mediated activation of pyramidal cells.

Antidepressants are ineffective in healthy probands [54] and show less robust or no behavioral effects in physiologically normal, unstressed animals [5, 10], which raised the question of whether SST IN-mediated activation of PNs required prior chronic stress exposure. To address this possibility, we repeated the above c-Fos and FosB reporter assays in unstressed mice (Fig. 4E), using quadruple immunostaining for the SST IN marker mCherry, PV, c-Fos, and FosB. Separate quantitation of c-Fos$^+$ mCherry$^+$ and FosB$^+$ mCherry$^+$ doubly-positive SST INs in the PLC of hM3Dq vs. Ctrl virus-injected mice confirmed that hM3Dq plus CNO led to activation of SST INs in unstressed mice (Fig. 4F1–F2). The density of c-Fos plus FosB-doubly positive putative PNs (quantified as c-Fos$^+$ and FosB$^+$ cells that were negative for mCherry and PV) was also increased in hM3Dq vs. Ctrl injected mice (Fig. 4F3). However, post hoc analyses indicated that the virus effect was significant only for FosB- and not c-Fos-expressing PNs (Fig. 4F3). The density of c-Fos$^+$ PV INs was unchanged, indicating once again that disinhibition of PNs by inhibition of PV cells did not contribute to the activation of PNs (Fig. 4F4). Scoring of c-Fos and FosB doubly-positive putative PNs indicated that ~26% of c-Fos$^+$ cells were positive for FosB, while ~20% of FosB-expressing cells also expressed c-Fos. Therefore, the data suggest that there are two distinct and similarly abundant populations of PNs that responded differently to chronic stress exposure. A first population of PNs characterized by the expression of c-Fos was activated by SST INs selectively after chronic stress exposure of mice. A second population of PNs characterized by expression of FosB was activated by SST neurons independent of stress exposure. Possible mechanisms underlying SST IN-mediated activation of these two populations of PNs are discussed.

## DISCUSSION

Here, we used a novel chronic chemogenetic approach to map GABAergic neural circuits that mediate antidepressant drug-like behavioral changes, including resilience to the anxiogenic and anhedonia-like changes of chronic stress and reversal of chronic stress-induced behavioral effects. As a first major finding, we report that SST INs in the PLC mediate such responses in males but not females, while functionally homologous SST INs in the vHPC mediate such responses in female but not male mice. In contrast to the pro-resilience effects of SST neurons, we found that increased PV neuron activity has detrimental effects in that it exacerbates anxiety and anhedonia-like behavior in stress-exposed animals. Long-range inputs from the mPFC [55] and vHPC [56] to the amygdala and nucleus accumbens are known to contribute to the top-down control of anxiety and anhedonia-related changes in motivated behaviors, and they are both known to be highly sensitive to chronic stress exposure. The mPFC and vHPC are also similarly vulnerable to stress and are known as critical substrates mediating the detrimental effects of chronic stress exposure [1]. Our data reveal striking sex differences in the relative importance of GABAergic microcircuits in the mPFC and vHPC in regulating their subcortical target areas. Importantly, we recently described sex differences in mPFC-mediated stress resilience using a transcriptomic approach. The mPFC of male but not female mice with disinhibited SST neurons (SSTCre:$\gamma2^{f/f}$ mice) is associated with resilience to chronic stress-induced transcriptome changes, suggesting that stress resilience and sex differences in the mechanism underlying stress resilience map to SST neurons [46]. Whether the same applies to SST neurons in the vHPC will require further experimentation. An alternate candidate hippocampal circuit may involve projections from the subiculum to the bed nucleus of the stria terminalis that encode female-specific chronic stress-induced anxiety [57].

As a second significant finding, we report that the antidepressant-like, CVS-reversing behavioral consequences of SST IN activation are associated with increased rather than reduced activity of their putative PN targets. This was surprising because there is plenty of evidence that SST INs inhibit their target cells. First, the antidepressant-like behavioral phenotype of mice with disinhibited SST INs is associated with strengthened inhibitory synaptic inputs onto PNs [36]. Second, acute stimulation of Martinotti-type SST cells is widely known to hyperpolarize PNs [53] and to reduce dendritic $Ca^{2+}$ influx [51, 58, 59], while acute inactivation of Martinotti cells leads to disinhibition and action potential firing of PNs [53]. However, in support of our findings, optogenetic stimulation of PNs in the mPFC is known to mimic antidepressant drug-induced behavioral effects [17–20, 60–62].

The large majority of neocortical SST INs (layers 2/3 and 5) target the distal apical dendrites of pyramidal cells. However, a morphologically distinct subgroup of SST cells in cortical layer IV predominantly inhibits $PV^{+}$ INs, which leads to disinhibition of principal cells [53]. These findings raised the possibility that SST-neuron-mediated activation of pyramidal cells could involve PV-IN-mediated disinhibition. However, using c-Fos as a reporter of neural activity, we found no evidence indicating SST IN-mediated inhibition of PV INs.

Our study should also help resolve the apparent paradox that increased inhibition and increased excitation can both have detrimental consequences and, in other situations, turn out to be beneficial. Increased pyramidal cell activity in the mPFC is associated with antidepressant effects, but seemingly only if the activity is increased in moderation and accompanied by enhanced feedback inhibition. If feedback inhibition cannot be scaled up, such as in mice with a genetically induced reduction in postsynaptic $GABA_A$ receptors (*Gabrg2*$^{+/-}$ mice), the resulting increased activation of glutamatergic neurons is detrimental as it fails to be compensated by increased feedback inhibition [10]. The chronically enhanced excitation then results in LTD-like downregulation of excitatory postsynapses on PNs, which results in reduced connectivity of neurons and is reflected in an anxiety- and depressive-like phenotype [10]. By contrast, SST IN-mediated activation of PNs in the present study appears to be self-limiting since excessive activation of SST neurons would inhibit rather than further increase the activity of pyramidal cells.

It is further necessary to consider whether a change in synaptic excitation-inhibition ratios is limited to the dendritic compartment or includes the soma and AIS region of pyramidal cells. Our study demonstrates that increasing inhibition at dendrites leads to stress resilience in a sex-specific manner. By contrast, inhibition of PNs by PV cells via axo-somatic and axo-AIS synapses has detrimental effects with opposite sex specificity, as shown for stress-induced anxiety due to hyperactivity of PV cells in the mPFC of female and hippocampus of male mice [49, 50]. We have demonstrated that chemogenetic stimulation of PV cells in the mPFC of males replicates the detrimental effects seen naturally in stress-exposed females. Therefore, even though chronic stress does not normally lead to significant hyperactivity of PV cells in the mPFC of males, the detrimental downstream effects of PV hyperactivity are conserved across the sexes.

When designing our chemogenetic stimulation protocol, we reasoned that drastically increasing GABAergic dendritic inhibition would interfere with activity-dependent plasticity at dendrites needed to increase the activity of target cells, as evidenced by the lack of antidepressant efficacy of benzodiazepines [63]. Accordingly, we chose a low concentration of CNO (~0.2 mg/kg/h) at, if not below, the threshold required for measurable hM3Dq-induced changes in neural activity in vitro [64]. Future experiments will need to establish the optimal level of SST neuron activation for the most effective reversal of chronic stress effects.

Our data provide a mechanistic rationale for the lack of antidepressant efficacy of benzodiazepines [63], which predominantly potentiate $GABA_A$ receptors underlying phasic inhibition. Benzodiazepines enhance inhibition indiscriminately at dendrites, soma, and AIS of virtually all neurons along the neuraxis, which underlies their rapid action as anxiolytics, sedatives, and myorelaxants [65]. However, studies in mice indicate that chronically increased inhibition of PNs at the soma and AIS by PV INs has detrimental effects. On the contrary, we show that selective chronic inhibition at dendrites of PNs by SST-INs, most likely through α5-$GABA_A$ receptors [60, 66] (perhaps with a contribution of α2-$GABA_A$ receptors [67]), holds promise as a target for antidepressants [61, 68]. Accordingly, we propose that SST INs are acutely neuro-protective during stress exposure and correspondingly high network load by limiting NMDA receptor-mediated $Ca^{2+}$ influx into dendrites via activation of postsynaptic $GABA_A$ receptors [58, 66]. This mechanism of GABAergic inhibition would be potentiated by benzodiazepines, which are known to be acutely neuroprotective [69, 70]. Subsequently, SST IN activation in between and after stressful periods facilitates the recovery of PNs through potentiation of tonic inhibition, which paradoxically increases the excitability of PNs. As a possible mechanism, tonic inhibition of dendrites through α5-$GABA_A$ receptors has been shown to lead to de-inactivation of t-type voltage-gated $Ca^{2+}$ channels, which then increases dendritic excitability and pyramidal cell output [60]. Benzodiazepine-mediated potentiation of postsynaptic $GABA_A$ receptors and corresponding strong hyperpolarization at dendrites and the soma and AIS is likely to override SST IN-mediated activation of PNs at dendrites, which explains the absence of antidepressant properties.

We showed that SST IN-mediated activation of at least 30% of PNs in the PLC requires prior stress exposure of the animals. These PNs expressed c-Fos and lacked detectable FosB expression in unstressed animals. By extension, SST IN-mediated activation of c-Fos-expressing PNs in chronically stressed animals may require a depolarizing shift in the $Cl^{-}$-reversal potential, which renders $GABA_A$ receptor-mediated inhibition less effective or even

excitatory [71, 72]. Alternatively, SST IN-mediated activation of c-Fos-expressing PNs may involve de-inactivation of t-type $Ca^{2+}$ channels that were subject to stress-induced inactivation. These two mechanisms could operate simultaneously at somatic and dendritic GABAergic synapses, respectively. We also cannot exclude contributions by chronic stress-dependent forms of plasticity of glutamatergic synapses [73, 74]. Lastly, it is essential to consider that chronically increased activity of SST INs may increase the release of SST (which has anxiolytic and antidepressant properties [75]) and enhance GABA signaling via $GABA_B$ receptors [76]. However, these mechanisms have inhibitory effects on PNs and, therefore, seem unlikely to contribute to the mechanism described here.

Notably, although the brain substrate for GABA-mediated neuroprotective and antidepressant effects is strikingly sex-specific, similar properties of dendrite-targeting SST INs in the PLC and vHPC, along with the shared subcortical targets of these brain regions, should allow dendrite targeting antidepressant therapies to be efficacious independent of sex.

## REFERENCES

1. Duman RS, Malberg J, Thome J. Neural plasticity to stress and antidepressant treatment. Biol Psychiatry. 1999;46:1181–91.
2. Fogaca MV, Duman RS. Cortical GABAergic dysfunction in stress and depression: new insights for therapeutic interventions. Front Cell Neurosci. 2019;13:87.
3. Luscher B, Shen Q, Sahir N. The GABAergic deficit hypothesis of major depressive disorder. Mol Psychiatry. 2011;16:383–406.
4. Luscher B, Fuchs T. GABAergic control of depression-related brain states. Adv Pharmacol. 2015;73:97–144.
5. Earnheart JC, Schweizer C, Crestani F, Iwasato T, Itohara S, Mohler H, et al. GABAergic control of adult hippocampal neurogenesis in relation to behavior indicative of trait anxiety and depression states. J Neurosci. 2007;27:3845–54.
6. Shen Q, Lal R, Luellen BA, Earnheart JC, Andrews AM, Luscher B. gamma-Aminobutyric acid-type A receptor deficits cause hypothalamic-pituitary-adrenal axis hyperactivity and antidepressant drug sensitivity reminiscent of melancholic forms of depression. Biol Psychiatry. 2010;68:512–20.
7. Sanacora G, Mason GF, Rothman DL, Krystal JH. Increased occipital cortex GABA concentrations in depressed patients after therapy with selective serotonin reuptake inhibitors. Am J Psychiatry. 2002;159:663–5.
8. Sanacora G, Mason GF, Rothman DL, Hyder F, Ciarcia JJ, Ostroff RB, et al. Increased cortical GABA concentrations in depressed patients receiving ECT. Am J Psychiatry. 2003;160:577–9.
9. Perrine SA, Ghoddoussi F, Michaels MS, Sheikh IS, McKelvey G, Galloway MP. Ketamine reverses stress-induced depression-like behavior and increased GABA levels in the anterior cingulate: an 11.7 T 1H-MRS study in rats. Prog Neuropsychopharmacol Biol Psychiatry. 2014;51:9–15.
10. Ren Z, Pribiag H, Jefferson SJ, Shorey M, Fuchs T, Stellwagen D, et al. Bidirectional homeostatic regulation of a depression-related brain state by gamma-aminobutyric acidergic deficits and ketamine treatment. Biol Psychiatry. 2016;80:457–68.
11. Ghosal S, Duman CH, Liu RJ, Wu M, Terwilliger R, Girgenti MJ, et al. Ketamine rapidly reverses stress-induced impairments in GABAergic transmission in the prefrontal cortex in male rodents. Neurobiol Dis. 2020;134:104669.
12. Luscher B, Feng M, Jefferson SJ. Antidepressant mechanisms of ketamine: focus on GABAergic inhibition. Adv Pharmacol. 2020;89:43–78.
13. Tan T, Wang W, Liu T, Zhong P, Conrow-Graham M, Tian X, et al. Neural circuits and activity dynamics underlying sex-specific effects of chronic social isolation stress. Cell Rep. 2021;34:108874.
14. Holmes SE, Scheinost D, Finnema SJ, Naganawa M, Davis MT, DellaGioia N, et al. Lower synaptic density is associated with depression severity and network alterations. Nat Commun. 2019;10:1529.
15. Drysdale AT, Grosenick L, Downar J, Dunlop K, Mansouri F, Meng Y, et al. Resting-state connectivity biomarkers define neurophysiological subtypes of depression. Nat Med. 2017;23:28–38.
16. Duman RS, Sanacora G, Krystal JH. Altered connectivity in depression: GABA and glutamate neurotransmitter deficits and reversal by novel treatments. Neuron. 2019;102:75–90.
17. Covington HE 3rd, Lobo MK, Maze I, Vialou V, Hyman JM, Zaman S. Antidepressant effect of optogenetic stimulation of the medial prefrontal cortex. J Neurosci. 2010;30:16082–90.
18. Fuchikami M, Thomas A, Liu R, Wohleb ES, Land BB, DiLeone RJ, et al. Optogenetic stimulation of infralimbic PFC reproduces ketamine's rapid and sustained antidepressant actions. Proc Natl Acad Sci USA. 2015;112:8106–11.
19. Ferenczi EA, Zalocusky KA, Liston C, Grosenick L, Warden MR, Amatya D, et al. Prefrontal cortical regulation of brainwide circuit dynamics and reward-related behavior. Science. 2016;351:aac9698.
20. Hare BD, Shinohara R, Liu RJ, Pothula S, DiLeone RJ, Duman RS. Optogenetic stimulation of medial prefrontal cortex Drd1 neurons produces rapid and long-lasting antidepressant effects. Nat Commun. 2019;10:223.
21. Kornstein SG, Schatzberg AF, Thase ME, Yonkers KA, McCullough JP, Keitner GI, et al. Gender differences in chronic major and double depression. J Affect Disord. 2000;60:1–11.
22. Seney ML, Glausier J, Sibille E. Large-scale transcriptomics studies provide insight into sex differences in depression. Biol Psychiatry. 2022;91:14–24.
23. Dienel SJ, Fish KN, Lewis DA. The nature of prefrontal cortical GABA neuron alterations in schizophrenia: markedly lower somatostatin and parvalbumin gene expression without missing neurons. Am J Psychiatry. 2023;180:495–507.
24. Prevot T, Sibille E. Altered GABA-mediated information processing and cognitive dysfunctions in depression and other brain disorders. Mol Psychiatry. 2021;26:151–67.
25. Rudy B, Fishell G, Lee S, Hjerling-Leffler J. Three groups of interneurons account for nearly 100% of neocortical GABAergic neurons. Dev Neurobiol. 2011;71:45–61.
26. Karnani MM, Jackson J, Ayzenshtat I, Hamzehei Sichani A, Manoocheri K, Kim S, et al. Opening holes in the blanket of inhibition: localized lateral disinhibition by VIP interneurons. J Neurosci. 2016;36:3471–80.
27. Yao Z, van Velthoven CTJ, Nguyen TN, Goldy J, Sedeno-Cortes AE, Baftizadeh F, et al. A taxonomy of transcriptomic cell types across the isocortex and hippocampal formation. Cell. 2021;184:3222–41.e3226.
28. Booker SA, Vida I. Morphological diversity and connectivity of hippocampal interneurons. Cell Tissue Res. 2018;373:619–41.
29. Pittenger C, Duman RS. Stress, depression, and neuroplasticity: a convergence of mechanisms. Neuropsychopharmacology. 2008;33:88–109.
30. Holmes SE, Finnema SJ, Naganawa M, DellaGioia N, Holden D, Fowles K, et al. Imaging the effect of ketamine on synaptic density (SV2A) in the living brain. Mol Psychiatry. 2022;27:2273–81.
31. Fee C, Banasr M, Sibille E. Somatostatin-positive gamma-aminobutyric acid interneuron deficits in depression: cortical microcircuit and therapeutic perspectives. Biol Psychiatry. 2017;82:549–59.
32. Harerimana NV, Liu Y, Gerasimov ES, Duong D, Beach TG, Reiman EM, et al. Genetic evidence supporting a causal role of depression in Alzheimer's disease. Biol Psychiatry. 2022;92:25–33.
33. Mathys H, Peng Z, Boix CA, Victor MB, Leary N, Babu S, et al. Single-cell atlas reveals correlates of high cognitive function, dementia, and resilience to Alzheimer's disease pathology. Cell. 2023;186:4365–85.e4327.
34. Joffe ME, Maksymetz J, Luschinger JR, Dogra S, Ferranti AS, Luessen DJ, et al. Acute restraint stress redirects prefrontal cortex circuit function through mGlu(5) receptor plasticity on somatostatin-expressing interneurons. Neuron. 2022;110:1068–83.e1065.
35. Pelkey KA, Chittajallu R, Craig MT, Tricoire L, Wester JC, McBain CJ. Hippocampal GABAergic Inhibitory Interneurons. Physiol Rev. 2017;97:1619–747.
36. Fuchs T, Jefferson SJ, Hooper A, Yee PH, Maguire J, Luscher B. Disinhibition of somatostatin-positive GABAergic interneurons results in an anxiolytic and antidepressant-like brain state. Mol Psychiatry. 2017;22:920–30.
37. Jefferson SJ, Feng M, Chon U, Guo Y, Kim Y, Luscher B. Disinhibition of somatostatin interneurons confers resilience to stress in male but not female mice. Neurobiol Stress. 2020;13:100238.
38. Paxinos G, Franklin K. Paxinos and Franklin's the mouse brain in stereotaxic coordinates. 4th ed. Amsterdam, Boston; Elsevier Academic Press; 2013.
39. LaPlant Q, Chakravarty S, Vialou V, Mukherjee S, Koo JW, Kalahasti G, et al. Role of nuclear factor kappaB in ovarian hormone-mediated stress hypersensitivity in female mice. Biol Psychiatry. 2009;65:874–80.
40. Labonte B, Engmann O, Purushothaman I, Menard C, Wang J, Tan C, et al. Sex-specific transcriptional signatures in human depression. Nat Med. 2017;23:1102–11.
41. Guilloux JP, Seney M, Edgar N, Sibille E. Integrated behavioral z-scoring increases the sensitivity and reliability of behavioral phenotyping in mice: relevance to emotionality and sex. J Neurosci Methods. 2011;197:21–31.
42. Feng M, Crowley NA, Patel A, Guo Y, Bugni SE, Luscher B. Reversal of a treatment-resistant, depression-related brain state with the Kv7 channel opener retigabine. Neuroscience. 2019;406:109–25.
43. Isingrini E, Camus V, Le Guisquet AM, Pingaud M, Devers S, Belzung C. Association between repeated unpredictable chronic mild stress (UCMS) procedures with a high fat diet: a model of fluoxetine resistance in mice. PLoS ONE. 2010;5:e10404.

44. Sun J, Yuan Y, Wu X, Liu A, Wang J, Yang S, et al. Excitatory SST neurons in the medial paralemniscal nucleus control repetitive self-grooming and encode reward. Neuron. 2022;110:3356–73.e3358.
45. Malkesman O, Scattoni ML, Paredes D, Tragon T, Pearson B, Shaltiel G, et al. The female urine sniffing test: a novel approach for assessing reward-seeking behavior in rodents. Biol Psychiatry. 2010;67:864–71.
46. Shao M, Botvinov J, Banerjee D, Girirajan S, Lüscher B. Transcriptome signatures of the medial prefrontal cortex underlying GABAergic control of resilience to chronic stress exposure. Mol Psychiatry. 2024, in press. https://doi.org/10.1101/2024.07.10.602959.
47. Muir J, Tse YC, Iyer ES, Biris J, Cvetkovska V, Lopez J, et al. Ventral hippocampal afferents to nucleus accumbens encode both latent vulnerability and stress-induced susceptibility. Biol Psychiatry. 2020;88:843–54.
48. Sohal VS, Rubenstein JLR. Excitation-inhibition balance as a framework for investigating mechanisms in neuropsychiatric disorders. Mol Psychiatry. 2019;24:1248–57.
49. Page CE, Shepard R, Heslin K, Coutellier L. Prefrontal parvalbumin cells are sensitive to stress and mediate anxiety-related behaviors in female mice. Sci Rep. 2019;9:19772.
50. Bhatti DL, Medrihan L, Chen MX, Jin J, McCabe KA, Wang W, et al. Molecular and cellular adaptations in hippocampal parvalbumin neurons mediate behavioral responses to chronic social stress. Front Mol Neurosci. 2022;15:898851.
51. Murayama M, Perez-Garci E, Nevian T, Bock T, Senn W, Larkum ME. Dendritic encoding of sensory stimuli controlled by deep cortical interneurons. Nature. 2009;457:1137–41.
52. Miyata S, Tsujioka H, Itoh M, Matsunaga W, Kuramoto H, Kiyohara T. Time course of Fos and Fras expression in the hypothalamic supraoptic neurons during chronic osmotic stimulation. Brain Res Mol Brain Res. 2001;90:39–47.
53. Xu H, Jeong HY, Tremblay R, Rudy B. Neocortical somatostatin-expressing GABAergic interneurons disinhibit the thalamorecipient layer 4. Neuron. 2013;77:155–67.
54. Reed JL, Nugent AC, Furey ML, Szczepanik JE, Evans JW, Zarate CA Jr. Effects of ketamine on brain activity during emotional processing: differential findings in depressed versus healthy control participants. Biol Psychiatry Cogn Neurosci Neuroimaging. 2019;4:610–8.
55. Jacobs DS, Moghaddam B. Medial prefrontal cortex encoding of stress and anxiety. Int Rev Neurobiol. 2021;158:29–55.
56. Baimel C, Jang E, Scudder SL, Manoocheri K, Carter AG. Hippocampal-evoked inhibition of cholinergic interneurons in the nucleus accumbens. Cell Rep. 2022;40:111042.
57. Miller CN, Li Y, Beier KT, Aoto J. Acute stress causes sex-dependent changes to ventral subiculum synapses, circuitry, and anxiety-like behavior. bioRxiv, https://doi.org/10.1101/2024.08.02.606264.
58. Chiu CQ, Lur G, Morse TM, Carnevale NT, Ellis-Davies GC, Higley MJ. Compartmentalization of GABAergic inhibition by dendritic spines. Science. 2013;340:759–62.
59. Schulz JM, Knoflach F, Hernandez MC, Bischofberger J. Enhanced dendritic inhibition and impaired NMDAR activation in a mouse model of down syndrome. J Neurosci. 2019;39:5210–21.
60. Chiu CQ, Morse TM, Nani F, Knoflach F, Hernandez M-C, Jadi M, et al. Tonic GABAergic activity facilitates dendritic calcium signaling and short-term plasticity. bioRxiv. https://doi.org/10.1101/2020.04.22.055137.
61. Luscher B, Maguire JL, Rudolph U, Sibille E. GABA(A) receptors as targets for treating affective and cognitive symptoms of depression. Trends Pharmacol Sci. 2023;44:586–600.
62. Prevot T, Bernardo A, Lee P, Marcotte M, Knutson D, Sharmin D, et al. Positive allosteric modulation at α5-GABAA receptor reverses cognitive dysfunctions and neuronal atrophy in mouse model of chronic stress. Biol Psychiatry. 2021;89:S213–S214.
63. Benasi G, Guidi J, Offidani E, Balon R, Rickels K, Fava GA. Benzodiazepines as a monotherapy in depressive disorders: a systematic review. Psychother Psychosom. 2018;87:65–74.
64. Alexander GM, Rogan SC, Abbas AI, Armbruster BN, Pei Y, Allen JA, et al. Remote control of neuronal activity in transgenic mice expressing evolved G protein-coupled receptors. Neuron. 2009;63:27–39.
65. Engin E, Benham RS, Rudolph U. An emerging circuit pharmacology of GABAA receptors. Trends Pharmacol Sci. 2018;39:710–32.
66. Schulz JM, Knoflach F, Hernandez MC, Bischofberger J. Dendrite-targeting interneurons control synaptic NMDA-receptor activation via nonlinear alpha5-GABA(A) receptors. Nat Commun. 2018;9:3576.
67. Benham RS, Choi C, Hodgson NW, Hewage NB, Kastli R, Donahue RJ, et al. alpha2-containing gamma-aminobutyric acid type A receptors promote stress resiliency in male mice. Neuropsychopharmacology. 2021;46:2197–206.
68. Fee C, Prevot TD, Misquitta K, Knutson DE, Li G, Mondal P, et al. Behavioral deficits induced by somatostatin-positive GABA neuron silencing are rescued by alpha 5 GABA-A receptor potentiation. Int J Neuropsychopharmacol. 2021;24:505–18.
69. Sarnowska A, Beresewicz M, Zablocka B, Domanska-Janik K. Diazepam neuroprotection in excitotoxic and oxidative stress involves a mitochondrial mechanism additional to the GABAAR and hypothermic effects. Neurochem Int. 2009;55:164–73.
70. Ooba S, Hasuo H, Shigemori M, Akasu T. Diazepam attenuates the post-traumatic hyperactivity of excitatory synapses in rat hippocampal CA1 neurons. Neurosci Res. 2008;62:195–205.
71. Hewitt SA, Wamsteeker JI, Kurz EU, Bains JS. Altered chloride homeostasis removes synaptic inhibitory constraint of the stress axis. Nat Neurosci. 2009;12:438–43.
72. MacKenzie G, Maguire J. Chronic stress shifts the GABA reversal potential in the hippocampus and increases seizure susceptibility. Epilepsy Res. 2015;109:13–27.
73. Thompson SM, Kallarackal AJ, Kvarta MD, Van Dyke AM, LeGates TA, Cai X. An excitatory synapse hypothesis of depression. Trends Neurosci. 2015;38:279–94.
74. Yuen EY, Wei J, Liu W, Zhong P, Li X, Yan Z. Repeated stress causes cognitive impairment by suppressing glutamate receptor expression and function in prefrontal cortex. Neuron. 2012;73:962–77.
75. Engin E, Stellbrink J, Treit D, Dickson CT. Anxiolytic and antidepressant effects of intracerebroventricularly administered somatostatin: behavioral and neurophysiological evidence. Neuroscience. 2008;157:666–76.
76. Watson TC, Booker SA. Somatostatin interneurons recruit pre- and postsynaptic GABA(B) receptors in the adult mouse dentate gyrus. eNeuro 2024;11:ENEURO.0115-0124.2024.

## ACKNOWLEDGEMENTS

We thank Yao Guo for her expert technical assistance and Meiyu Shao for discussions and carefully reading the manuscript. This publication was made possible by a grant (MH099851) from the National Institute of Mental Health (NIMH) to BL and generous support from Penn State University. Its contents are solely the responsibility of the authors and do not necessarily represent the views of Penn State or the NIMH.

## COMPETING INTERESTS

The authors declare no competing interests.

## ADDITIONAL INFORMATION

**Supplementary information** The online version contains supplementary material available at https://doi.org/10.1038/s41380-024-02835-8.

**Correspondence** and requests for materials should be addressed to Bernhard Lüscher.